


Experimental investigation of amplification, via a mechanical delay-line, in a rainbow-based metamaterial for energy harvesting

Cite as: Appl. Phys. Lett. **117**, 143902 (2020); <https://doi.org/10.1063/5.0023544>

Submitted: 30 July 2020 • Accepted: 20 September 2020 • Published Online: 06 October 2020

 J. M. De Ponti,  A. Colombi,  E. Riva, et al.

COLLECTIONS

 This paper was selected as Featured



View Online



Export Citation



CrossMark

ARTICLES YOU MAY BE INTERESTED IN

[Acoustic energy harvesting based on a planar acoustic metamaterial](#)

Applied Physics Letters **108**, 263501 (2016); <https://doi.org/10.1063/1.4954987>

[Phononic crystal Luneburg lens for omnidirectional elastic wave focusing and energy harvesting](#)

Applied Physics Letters **111**, 013503 (2017); <https://doi.org/10.1063/1.4991684>

[Metamaterial beam for flexural wave resonance rainbow trapping and piezoelectric energy harvesting](#)

Journal of Applied Physics **129**, 064505 (2021); <https://doi.org/10.1063/5.0040029>

Lock-in Amplifiers
up to 600 MHz



Zurich
Instruments



Experimental investigation of amplification, via a mechanical delay-line, in a rainbow-based metamaterial for energy harvesting

Cite as: Appl. Phys. Lett. **117**, 143902 (2020); doi: 10.1063/5.0023544

Submitted: 30 July 2020 · Accepted: 20 September 2020 ·

Published Online: 6 October 2020



View Online



Export Citation



CrossMark

J. M. De Ponti,^{1,2,a)}  A. Colombi,³  E. Riva,²  R. Ardito,¹  F. Braghin,²  A. Corigliano,¹  and R. V. Craster^{4,5,6} 

AFFILIATIONS

¹Department of Civil and Environmental Engineering, Politecnico di Milano, Piazza Leonardo da Vinci 32, 20133 Milano, Italy

²Department of Mechanical Engineering, Politecnico di Milano, Via Giuseppe La Masa 1, 20156 Milano, Italy

³Department of Civil, Environmental, and Geomatic Engineering, ETH, Stefano-Franscini-Platz, 5 8093 Zürich, Switzerland

⁴Department of Mathematics, Imperial College London, London SW7 2AZ, United Kingdom

⁵Department of Mechanical Engineering, Imperial College London, London SW7 2AZ, United Kingdom

⁶UMI 2004 Abraham de Moivre-CNRS, Imperial College London, London SW7 2AZ, United Kingdom

^{a)} Author to whom correspondence should be addressed: jacopomaria.deponti@polimi.it

ABSTRACT

We experimentally demonstrate that a rainbow-based metamaterial, created by a graded array of resonant rods attached to an elastic beam, operates as a mechanical delay-line by slowing down surface elastic waves to take advantage of wave interaction with resonance. Experiments demonstrate that the rainbow effect reduces the amplitude of the propagating wave in the host structure. At the same time, it dramatically increases both the period of interaction between the waves and the resonators and the wavefield amplitude in the rod endowed with the harvester. Increased energy is thus fed into the resonators over time: we show the enhanced energy harvesting capabilities of this system.

© 2020 Author(s). All article content, except where otherwise noted, is licensed under a Creative Commons Attribution (CC BY) license (<http://creativecommons.org/licenses/by/4.0/>). <https://doi.org/10.1063/5.0023544>

The opportunity to realize novel metamaterial devices in mechanics has recently attracted growing interest within the research community. In the context of elastic waves, considerable effort has been devoted to the investigation of novel wave control mechanisms motivated by the numerous applications of technological relevance involving vibrations, such as nondestructive evaluation,^{1,2} isolation,^{3,4} acoustic absorption,^{5,6} and wave enhancement and manipulation.^{7–11}

Metamaterials are often employed in combination to create multi-physics materials that leverage energy conversion phenomena between mechanical deformations and, for instance, electrical stimuli via piezoelectric coupling. This strategy has been exploited in the past to obtain multifunctional devices.¹² In this context, among the promising functionalities of acoustic metamaterials, focusing and mirroring of energy^{13,14} have been successfully employed for flexural waves^{15,16} and extended to vibration energy harvesting using piezoelectric materials.^{17–20}

A versatile way to manipulate elastic surface waves leverages graded metasurfaces, which are structures incorporating the gentle variation of resonating elements placed on, or within, the surface. This modulation strategy was conceived, and functionally designed, to

achieve broadband and efficient performance in deep elastic substrates (half-spaces) for surface elastic Rayleigh wave trapping^{21,22} through a phenomenon generally known in physics as the *rainbow effect*.^{23–25} A peculiar characteristic of these systems is their mode conversion capability, allowing surface Rayleigh waves to hybridize into bulk shear^{21,22} and pressure²⁶ waves. These all rely upon grading the system and obtaining frequency selective spatial separation; initially explored in electromagnetism in order to tailor a negative-index “left-handed” waveguide,²³ the rainbow effect has been later investigated in acoustics,²⁷ water waves,²⁸ and fluid loaded plates,²⁹ amongst others.

A purely theoretical study³⁰ recently claimed high performance for a graded metamaterial³⁰ that was functionally designed to enhance the energy harvesting from a host structure; there were naturally assumptions such as linearity, and lack of losses, that could modify the performance of a real device. Here, we carefully explore these theoretical claims with a thorough investigation both numerically and experimentally of the wavefield and of the real harvesting performances of the device, which is of paramount importance for applications. The graded array of resonating rods is employed to manipulate the wave

propagation, by inducing a wavenumber transformation along the structure. This effect, on one hand, allows us to slow-down waves and *de facto* increases the interaction time between the wave and the harvester, clamped on the structure. On the other hand, the wavenumber transformation is accompanied by an amplitude decrease in the waveguide together with a strong amplification inside the rods. Leveraging the interplay of these two effects, namely, amplification in the resonators and deceleration in the host beam, we illustrate that, for a sufficiently long excitation time, the mechanical delay line is able to harvest six times the energy of a single harvester when they are attached to the same structure and at the same location.

We consider the graded metamaterial illustrated in Fig. 1(a), designed to comply with the sub-wavelength scale of locally resonant systems;³¹ this is constructed using an aluminum beam ($E_a = 70$ GPa, $\nu_a = 0.33$ and $\rho_a = 2710$ kg/m³), having thickness $h_1 = 10$ mm and width $b = 30$ mm, which is augmented by an array of $N = 30$ resonating rods of variable height and a square cross-sectional area of 5 mm \times 5 mm. The array of consecutive rods is separated by a constant lattice spacing of $l_i = 15$ mm, which is sub-wavelength compared to the operational frequencies of the device ($\lambda \simeq 14l_i$), and the array, of total length $l_2 = 435$ mm, is placed at $l_1 = 300$ mm from the input source [Fig. 1(a)].

The dynamical behavior of the overall system is controlled by tuning the longitudinal resonance of each rod to functionally provide filtering behavior for wave propagation and modified dispersion in the neighborhood of the resonance frequency. Here, the operational frequency of each resonator is smoothly varied along the beam length, and this slows down the wave propagation through the array increasing the interaction time between the wave and the structure, as shown in the schematic of Fig. 1(b); for the host beam, wave propagation can only be modified by the dispersive nature of the medium [Fig. 1(b),

red wave packet]; in contrast, a carefully designed metamaterial is able to dramatically decrease the speed of the wave [Fig. 1(b), black wave packet]. This behavior is critical in achieving efficient electromechanical energy conversion between an input source and a piezoelectric harvester [red and blue arrows in Fig. 1(a), respectively] mounted on one of the resonators, whose height is defined in order to have a continuous axial resonance frequency variation, which takes into account additional mass added by the cantilever beams and the piezoelectric patches.³⁰ Specifically, the harvester has been designed in order to couple the axial fundamental mode with the flexural one of the cantilevers [Fig. 1(a)].

Dispersion curves are an important tool in terms of understanding the mechanism and designing the array, and they are shown in Fig. 2(b), in which a unit cell dispersion relation is investigated for different rod heights $h_r = h_i + r(h_f - h_i)/N$ spanning the range between $h_i = 250$ mm and $h_f = 650$ mm. These dispersion curves are for an infinite array of identical rods, each of the same height and equally spaced, and this local dispersion behavior allows us to understand how the graded array operates at the local spatial position corresponding to each height; implicitly, the assumption is that the nearest neighbors dominate the behavior of each rod and that the grading is gradual. Each of the varying rod heights, h_r , yields different dispersion curves and, therefore, induces a different local wave speed, which is the hallmark of the rainbow effect. For an operating frequency in the neighborhood of $f = 2.05$ kHz, the modulation is, therefore, accompanied by a wavenumber transformation [highlighted with dashed lines in Fig. 2(b)] when the smooth modulation of the rod profiles is considered. i.e., when the parameter space $[h_i, h_f]$ is mapped within the physical space $x \in [l_1, l_1 + l_2]$. Consistent with the description using dispersion, the group velocity $c_g = \partial\omega/\partial\kappa$ is modified by changing rod heights and it is illustrated in Fig. 2(b) through solid lines.

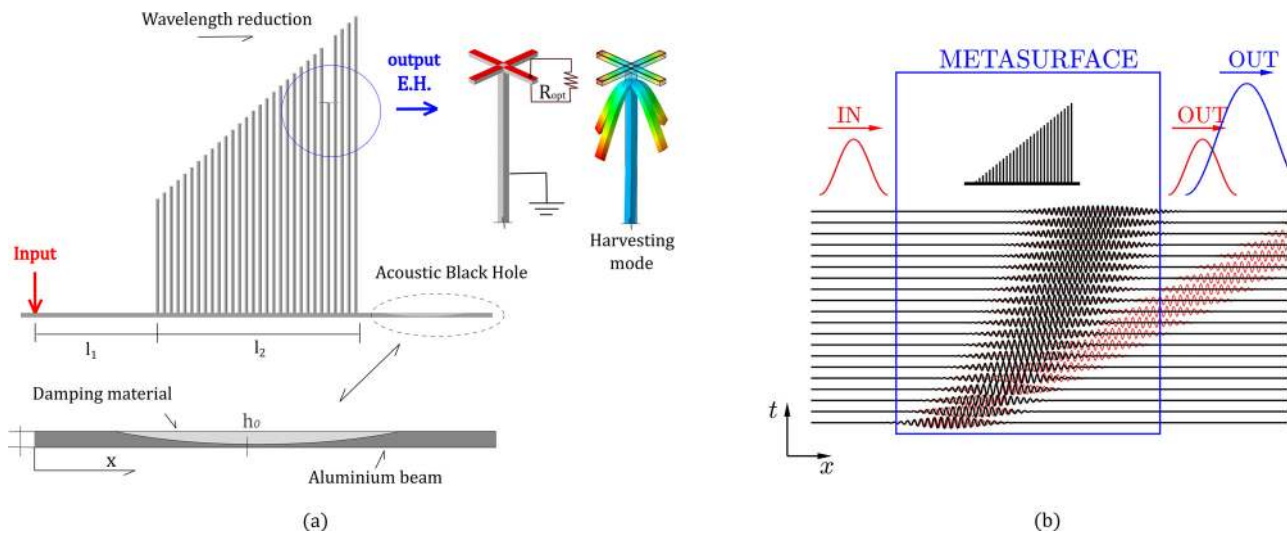


FIG. 1. (a) Schematic of the system. The rainbow device is made of an array of resonant rods covering a length depicted by l_2 , which are clamped on a host beam. The input region is represented in red and it is located at a distance l_1 from the array. The output region, corresponding to a rod equipped with four piezo-augmented cantilever beams arranged in a cross-like shape, is represented in blue. Each piezoelectric patch is connected to a resistive load R_{opt} , and the harvesting mode couples the axial elongation of the rod with the flexural deformation of the cantilevers. In the bottom part of the figure, a detailed view of an acoustic black hole that emulates absorbing boundary conditions is shown. (b) Schematic of the desired metamaterial effect on the wave propagation. The red wave packet is a schematic representation of the output achievable through a conventional harvester, i.e., without metamaterial. The black wave packet represents the amplification that can be obtained through a rainbow device.

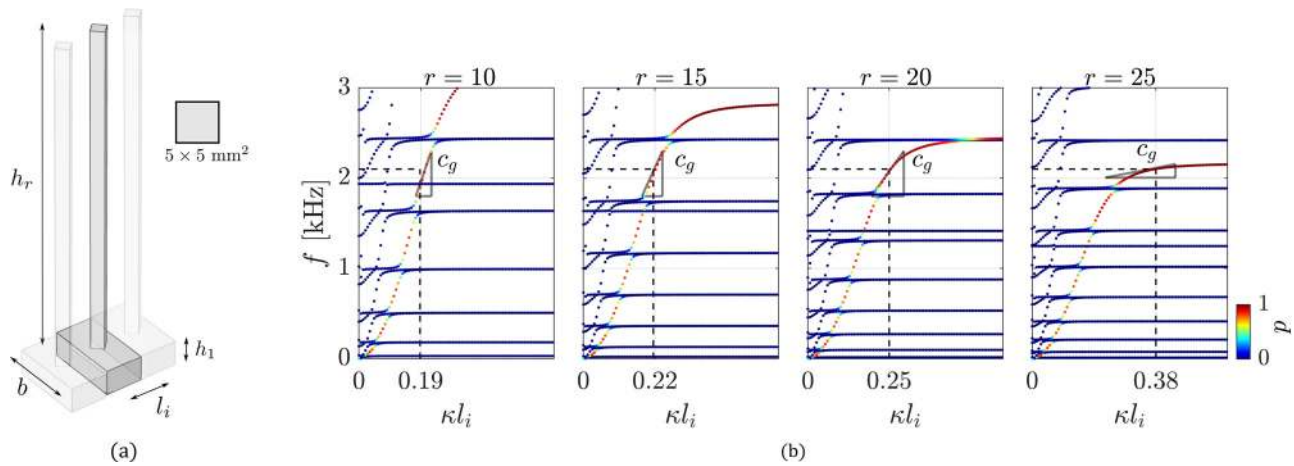


FIG. 2. (a) Schematic of the unit cell. (b) Dispersion relation associated with the unit cell made of the host beam equipped with the r th resonator, obtained using COMSOL Multiphysics[®]. The colors represent the wave polarization factor $p = |w|^2 / (|w|^2 + |u|^2 + |v|^2)$ (where u , v , and w are the displacements in the x , y , and z directions, respectively), computed through numerical integration within the resonator spatial domain. The wavenumber and associated group velocity are highlighted in the neighborhood of the working frequency with dashed lines and solid lines, respectively. For each longitudinal resonant frequency spanned by array of rods, a longer interaction between the waves and the resonators is achieved by reducing the group velocity c_g , i.e., increasing the wavenumber.

Specifically, c_g decreases for the increasing height of the rods h_r , until it is nullified for the 27th resonator, which is a key observation and, hereafter, employed to enhance the harvested power of the 26th resonator. The final three resonators in the array have heights such that, at the operating frequency, we are in the bandgap and wave propagation is disallowed and this acts to prevent wave propagation away from the harvester. To be precise, the mechanism we have identified is rainbow reflection³² since the zero group velocity and the strong impedance contrast are achieved at the rod's resonant frequency, namely, at the bandgap opening.³³ Previous works on acoustic experiments³⁴ have demonstrated that a non-linear graded profile yields focusing with higher energy density when compared with a linear gradient. This could be similarly investigated in elasticity to increase the benefits in terms of energy conversion.

For the experimental setup, shown in Fig. 3, we have an array of resonators clamped on the host beam through a set of screws and spaced by $l_1 = 300$ mm from the left boundary. The applied torque during the assembly slightly modifies the axial resonance frequency of the rods, which is reduced of approximately 100 Hz with respect to the numerical prediction. At the left boundary, a LDS v406 electrodynamic shaker is rigidly connected to the beam, to provide excitation, and an accelerometer, PCB 352C33, is placed on the surface in order to measure the real acceleration induced by the shaker. The right boundary is endowed with an acoustic black hole to prevent any spurious reflections; it is achieved by gradually varying the beam thickness and through the addition of a dissipating material to emulate absorbing boundaries.^{35–37}

A piezoelectric PZT-5H harvester ($E_p = 61$ GPa, $\nu_p = 0.31$, $\rho_p = 7800$ kg/m³, dielectric constant $\epsilon_{33}^T/\epsilon_0 = 3500$, and piezoelectric coefficient $e_{31} = -9.2$ C/m²) is placed at the position of the 26th resonator and allows us to quantify the vibrational energy that is transduced during the experimental tests. Specifically, each of the four piezoelectric electrodes is independently attached to an optimal resistive load $R = 6.8$ k Ω , whereby the resulting voltage drop is acquired in real time.

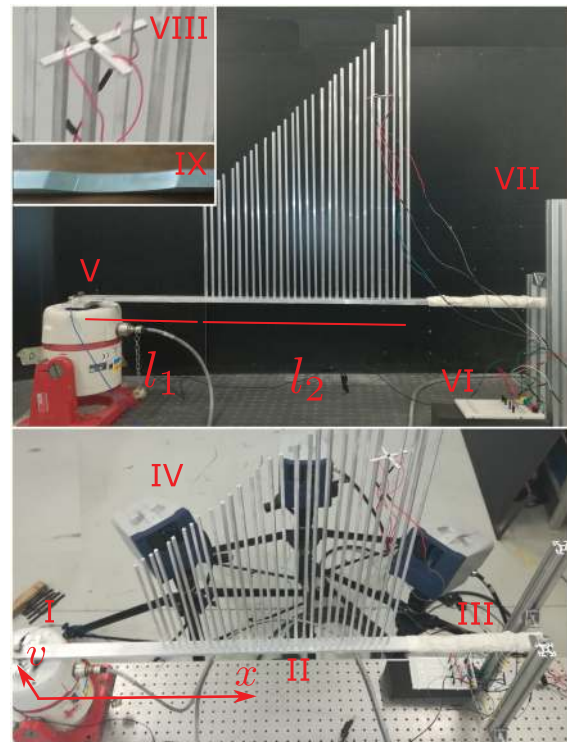


FIG. 3. Experimental setup. The excitation is provided through an electrodynamic shaker (I). The rainbow metamaterial is mounted on an otherwise plain beam (II) supplemented by an acoustic black hole (III), to prevent spurious reflections, and a 3D laser vibrometer used to measure the wavefield on the bottom surface of the beam (IV). The input acceleration is measured through an accelerometer located alongside the shaker (V), while the output power is measured by connecting the piezo-electrodes to a passive resistive load. The system is suspended through elastic cables located alongside the acoustic black hole (VII). A zoomed-in view of the harvester (VIII) and the acoustic black hole profile (IX) is shown in the inset.

The wavefield is measured on the bottom surface of the beam through a Polytec 3D Scanner Laser Doppler Vibrometer (SLDV), which is able to separate the out-of-plane velocity field in both space and time. A narrow-band spectrum excitation of central frequency at 2.05 kHz and width $\Delta f = 0.14$ kHz is synchronously started with the acquisition which, in turn, is averaged in time to decrease the noise. Two different testing conditions are considered: (a) only one resonator, equipped with the harvester, is placed on the beam and (b) all the resonators are present, whereby the metamaterial enables the wave speed control. This enables us to quantify the difference between a lone single harvester and the harvester embedded within the metamaterial.

The resulting velocity field, for the single rod, is illustrated in Fig. 4(a-I); since the beam is characterized by constant material properties along its main dimension, the associated wavelength is invariant

in space, as is clearly visible in the velocity profile in Fig. 4(a-II), corresponding to the time instant illustrated with the horizontal dashed line. In addition, at a generic point belonging to the beam, the imposed wave drops to zero after approximately 25 ms, which is highlighted in the vertical cut of the velocity field shown in Fig. 4(a-III).

The corresponding spectrogram is shown in Fig. 4(b); it is computed through a 2D Fourier Transform (FT) of the velocity field, properly windowed with a moving Gaussian function along x , which results in the function $\hat{v}_z(\kappa, x, f)$. The dependence upon frequency is eliminated by taking the RMS value in time, which allows us to define the spectrogram as the amplitude $|\hat{v}_z(\kappa, x)|$, displayed with colored contours in Fig. 4(b), confirming that wave propagation occurs without wavenumber transformation.³⁸ Turning to the harvester embedded within the metamaterial, the effect of the metamaterial is visible in Fig. 4(c-I) and in the corresponding horizontal [Fig. 4(c-II)] and

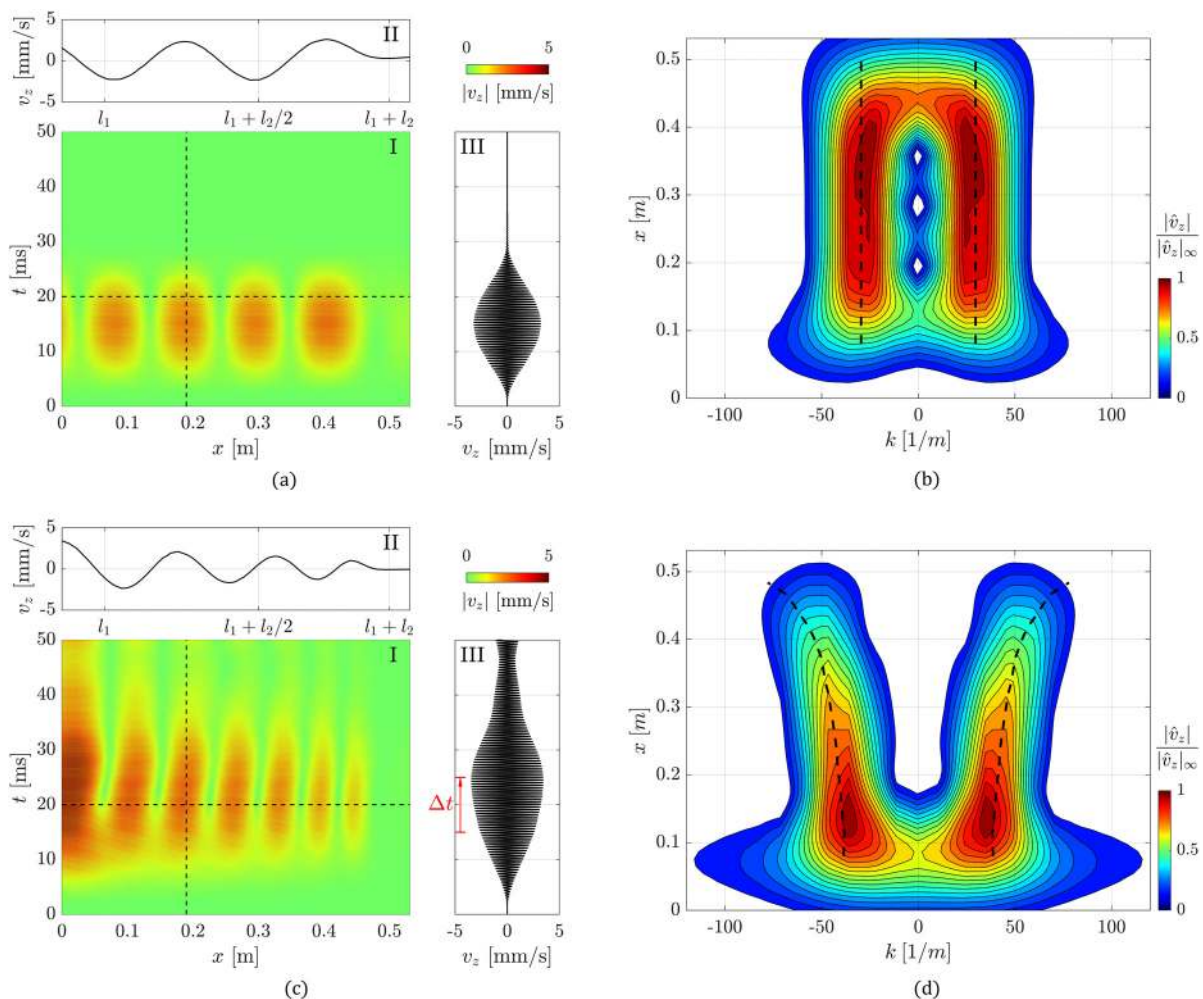


FIG. 4. Experimental velocity field for a beam with (a) one resonating rod and (c) the metamaterial. The horizontal dashed lines are representative of the time instant $t = 20$ ms, corresponding to the wave profile displayed on the top of the figure (II); at this time instant, the typical pattern of nodes and antinodes characterizing a standing wave is visible. The vertical dashed line is representative of the temporal wave profile measured at $x = 0.2$ m and illustrated in the right side of the figure (III). Corresponding spectrograms for (b) single resonator and (d) the metamaterial, with superimposed numerical dispersion for constant frequency and different resonator heights (dashed black line). While for the single harvester, the wavenumber is constant in space, a relevant wavenumber transformation can be observed when the metamaterial is mounted on the beam.

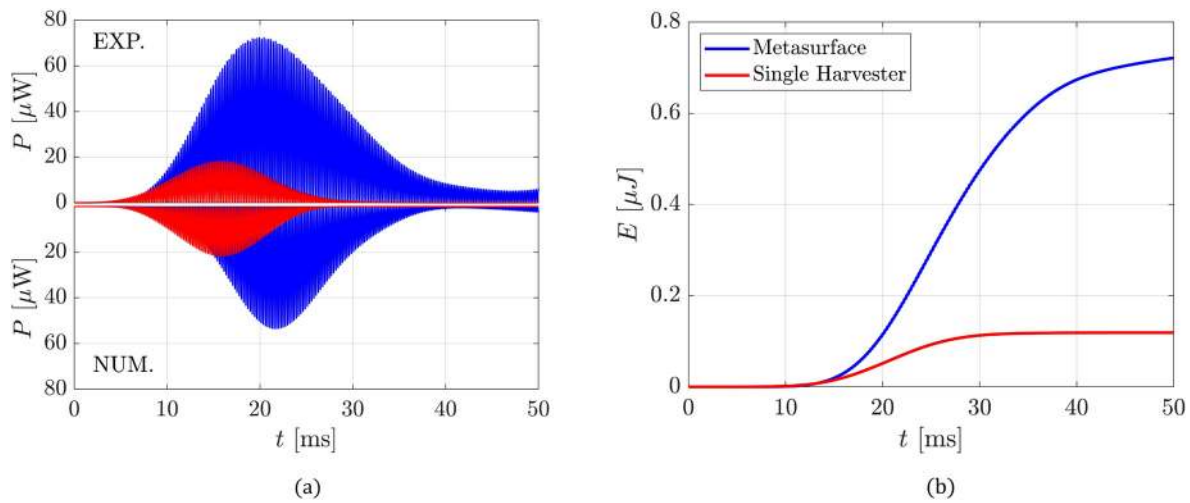


FIG. 5. (a) Numerical and experimental electric power produced by the harvester with (blue) and without (red) the metamaterial. (b) Experimental cumulated electric energy in time.

vertical [Fig. 4(c-III)] cuts. The associated wavelength varies along the x -direction of the host beam, whereby its variation is accompanied by amplitude decrease, as expected from the arguments presented earlier. We also observe that the temporal response is delayed and that the energy remains in the system for a longer time compared to the single harvester, which further enhances the metamaterial effect. This effect is created by the partial wave scattering and wave confinement occurring inside the array, and this is further confirmed by comparison between the expected wavenumber transformation (obtained with the numerical model and represented with black dashed lines) and the experimental spectrogram in Fig. 4(d). Finally, we quantify the energy harvesting capabilities of the system by comparing the experimental power output for the host beam with one resonator (red line) and the power achieved through the metamaterial effect (blue line), as shown in Fig. 5(a) (top), for the same excitation level. It is demonstrated that, thanks to the careful design of the array of rods, the wave propagation in the host beam is slowed down. As a result, a greater interaction time between the wave and the harvester and a wave localization responsible for a field amplification on the rod endowed with the harvester are guaranteed. This process reflects into a greater and delayed power output.

In addition to these experimental results, a comparison with the power calculated through a numerical simulation is shown in Fig. 5(a) (bottom). The system is numerically modeled through ABAQUS CAE 2018®, with a user subroutine introduced to include the electric resistance,^{39,40} and imposing the experimental acceleration time history. The output power is displayed in the bottom part of Fig. 5(a), for the case of one resonator (red) and of a full metamaterial (blue). The agreement between the experimental and the numerical data confirms that the rainbow effect is the observed mechanism and that the system is operating as we predict. The slightly different behavior between the experimental and numerical EH results could be attributed to several aspects, mainly connected to the effect of imperfections (rod heights, tightening of the screws) and to the experimental spurious reflections of the acoustic black hole that increase the energy confinement in the

host beam. As a matter of fact, the experimental/numerical agreement is more than satisfactory for the case of a single resonator, demonstrating the correctness of the model. For the case of the array, in which the number and the interplay of imperfections are by far larger than before, some differences arise. The investigation of all these aspects is out of the scope of this work but suggests future investigations on the defect sensitivity of the device.

The accumulated energy for the two scenarios, the lone harvester and the harvester embedded in the metamaterial, is then compared in Fig. 5(b) in the range of 0 – 50 ms, which corresponds to a total energy of 0.12 μJ and 0.72 μJ , demonstrating a strong increase in the harvesting capabilities. The advantage of the system is evident only after a certain amount of time and benefits from a sufficiently continuous, or long duration, source of excitation; if the excitation is discontinuous or very short, the metamaterial is less efficient.³⁰

In conclusion, we have experimentally demonstrated potential advantages in using a rainbow-based metamaterial for wave manipulation and energy harvesting. The metamaterial capability of slowing down waves enables a longer excitation of the resonators, which is then reflected in a higher electric power production. This behavior can be suitably employed for applications involving energy harvesting and can be scaled at the micro-scale for the implementation of next generation vibration energy harvesting devices.

See the [supplementary material](#) for a detailed description of the black hole geometry and energy harvesting details.

The authors wish to thank G. Borghi for the prototype realization. The Italian Ministry of Education, University and Research is acknowledged for the support provided through the Project “Department of Excellence LIS4.0-Lightweight and Smart Structures for Industry 4.0.” J.M.D.P thanks Politecnico di Milano for the scholarship on “Smart Materials and Metamaterials for industry 4.0.” R.V.C is funded by the UK Engineering and Physical Sciences Research Council (No. EP/T002654/1). This project has

also received funding from the European Union's Horizon 2020 Research and Innovation programme under Grant Agreement No. 863179 (Boheme).

DATA AVAILABILITY

The data that support the findings of this study are available from the corresponding author upon reasonable request.

REFERENCES

- ¹M. Molerón and C. Daraio, "Acoustic metamaterial for subwavelength edge detection," *Nat. Commun.* **6**, 8037 (2015).
- ²A. S. Gliozzi, M. Miniaci, F. Bosia, N. M. Pugno, and M. Scalrandi, "Metamaterials-based sensor to detect and locate nonlinear elastic sources," *Appl. Phys. Lett.* **107**, 161902 (2015).
- ³L. D'Alessandro, E. Belloni, R. Ardito, A. Corigliano, and F. Braghin, "Modeling and experimental verification of an ultra-wide bandgap in 3D phononic crystal," *Appl. Phys. Lett.* **109**, 221907 (2016).
- ⁴J. M. De Ponti, N. Paderno, R. Ardito, F. Braghin, and A. Corigliano, "Experimental and numerical evidence of comparable levels of attenuation in periodic and a-periodic metastructures," *Appl. Phys. Lett.* **115**, 031901 (2019).
- ⁵N. Jiménez, W. Huang, V. Romero-García, V. Pagneux, and J.-P. Groby, "Ultra-thin metamaterial for perfect and quasi-omnidirectional sound absorption," *Appl. Phys. Lett.* **109**, 121902 (2016).
- ⁶N. Jiménez, V. Romero-García, V. Pagneux, and J.-P. Groby, "Quasiperfect absorption by subwavelength acoustic panels in transmission using accumulation of resonances due to slow sound," *Phys. Rev. B* **95**, 014205 (2017).
- ⁷V. Romero-García, R. Picó, A. Cebrecos, V. J. Sánchez-Morcillo, and K. Staliunas, "Enhancement of sound in chirped sonic crystals," *Appl. Phys. Lett.* **102**, 091906 (2013).
- ⁸Y. Chen, H. Liu, M. Reilly, H. Bae, and M. Yu, "Enhanced acoustic sensing through wave compression and pressure amplification in anisotropic metamaterials," *Nat. Commun.* **5**, 5247 (2014).
- ⁹Y. Liu, Z. Liang, F. Liu, O. Diba, A. Lamb, and J. Li, "Source illusion devices for flexural lamb waves using elastic metasurfaces," *Phys. Rev. Lett.* **119**, 034301 (2017).
- ¹⁰P. Packo, A. N. Norris, and D. Torrent, "Inverse grating problem: efficient design of anomalous flexural wave reflectors and refractors," *Phys. Rev. Appl.* **11**, 014023 (2019).
- ¹¹X. Yan, R. Zhu, G. Huang, and F. G. Yuan, "Focusing guided waves using surface bonded elastic metamaterials," *Appl. Phys. Lett.* **103**, 121901 (2013).
- ¹²C. Sugino and A. Erturk, "Analysis of multifunctional piezoelectric metastructures for low-frequency bandgap formation and energy harvesting," *J. Phys. D: Appl. Phys.* **51**(21), 215103 (2018).
- ¹³R. V. Craster and S. Guenneau, *Acoustic Metamaterials, Negative Refraction, Imaging, Lensing and Cloaking* (Springer, 2012).
- ¹⁴G. J. Chaplain and R. V. Craster, "Flat lensing by graded line meta-arrays," *Phys. Rev. B* **99**, 220102(R) (2019).
- ¹⁵A. Colombi, P. Roux, S. Guenneau, and M. Rupin, "Directional cloaking of flexural waves in a plate with a locally resonant metamaterial," *J. Acoust. Soc. Am.* **137**, 1783 (2015).
- ¹⁶A. Colombi, "Resonant metalenses for flexural waves," *J. Acoust. Soc. Am.* **140**(5), EL423 (2016).
- ¹⁷S. Tol, F. L. Degertekin, and A. Erturk, "Structurally embedded reflectors and mirrors for elastic wave focusing and energy harvesting," *J. Appl. Phys.* **122**, 164503 (2017).
- ¹⁸S. Tol, F. L. Degertekin, and A. Erturk, "Phononic crystal Luneburg lens for omnidirectional elastic wave focusing and energy harvesting," *Appl. Phys. Lett.* **111**, 013503 (2017).
- ¹⁹A. Darabi and M. J. Leamy, "Analysis and experimental validation of an optimized gradient-index phononic-crystal lens," *Phys. Rev. Appl.* **10**, 024045 (2018).
- ²⁰M. Carrara, M. R. Cacan, J. Toussaint, M. Leamy, M. Ruzzene, and A. Erturk, "Metamaterial-inspired structures and concepts for elastoacoustic wave energy harvesting," *Smart Mater. Struct.* **22**, 065004 (2013).
- ²¹A. Colombi, D. Colquitt, P. Roux, S. Guenneau, and R. V. Craster, "A seismic metamaterial: The resonant metawedge," *Sci. Rep.* **6**, 27717 (2016).
- ²²A. Colombi, V. Ageeva, R. J. Smith, A. Clare, R. Patel, M. Clark, D. Colquitt, P. Roux, S. Guenneau, and R. V. Craster, "Enhanced sensing and conversion of ultrasonic Rayleigh waves by elastic metasurfaces," *Sci. Rep.* **7**, 6750 (2017).
- ²³K. L. Tsakmakidis, A. D. Boardman, and O. Hess, "Trapped rainbow storage of light in metamaterials," *Nature* **450**, 397–401 (2007).
- ²⁴D. Cardella, P. Celli, and S. Gonella, "Manipulating waves by distilling frequencies: A tunable shunt-enabled rainbow trap," *Smart Mater. Struct.* **25**, 085107 (2016).
- ²⁵P. Celli, B. Yousefzadeh, and C. Daraio, "S. Gonella Bandgap widening by disorder in rainbow metamaterials," *Appl. Phys. Lett.* **114**, 091903 (2019).
- ²⁶G. J. Chaplain, J. M. De Ponti, A. Colombi, R. Fuentes-Dominguez, P. Dryburg, D. Pieris, R. J. Smith, A. Clare, M. Clark, and R. V. Craster, "Tailored elastic surface to body wave Umklapp conversion," *Nat. Commun.* **11**, 3267 (2020).
- ²⁷J. Zhu, Y. Chen, X. Zhu, F. J. Garcia-Vidal, X. Yin, W. Zhang, and X. Zhang, "Acoustic rainbow trapping," *Sci. Rep.* **3**, 1728 (2013).
- ²⁸L. G. Bennetts, M. A. Peter, and R. V. Craster, "Graded resonator arrays for spatial frequency separation and amplification of water waves," *J. Fluid Mech.* **854**, R4 (2018).
- ²⁹E. A. Skelton, R. V. Craster, A. Colombi, and D. J. Colquitt, "The multi-physics metawedge: Graded arrays on fluid-loaded elastic plates and the mechanical analogues of rainbow trapping and mode conversion," *New J. Phys.* **20**, 053017 (2018).
- ³⁰J. M. De Ponti, A. Colombi, R. Ardito, F. Braghin, A. Corigliano, and R. V. Craster, "Graded elastic metasurface for enhanced energy harvesting," *New J. Phys.* **22**, 013013 (2020).
- ³¹A. Colombi, P. Roux, S. Guenneau, P. Gueguen, and R. V. Craster, "Forests as a natural seismic metamaterial: Rayleigh wave bandgaps induced by local resonances," *Sci. Rep.* **6**, 19238 (2016).
- ³²G. J. Chaplain, D. Pajer, J. M. De Ponti, and R. V. Craster, "Delineating rainbow reflection and trapping with applications for energy harvesting," *New J. Phys.* **22**, 063024 (2020).
- ³³M. Lott and P. Roux, "Effective impedance of a locally resonant metasurface," *Phys. Rev. Mater.* **3**, 6 065202 (2019).
- ³⁴A. Cebrecos, R. Picó, V. J. Sánchez-Morcillo, K. Staliunas, V. Romero-García, and L. M. Garcia-Raffi, "Enhancement of sound by soft reflections in exponentially chirped crystals," *AIP Adv.* **4**, 124402 (2014).
- ³⁵P. Rajagopal, M. Drozd, E. A. Skelton, M. J. S. Lowe, and R. V. Craster, "On the use of absorbing layers to simulate the propagation of elastic waves in unbounded isotropic media using commercially available finite element packages," *NDT E Int.* **51**, 30–40 (2012).
- ³⁶D. J. O'Boy, V. V. Krylov, and V. Kralovic, "Damping of flexural vibrations in rectangular plates using the acoustic black hole effect," *J. Sound Vib.* **329**, 22 (2010).
- ³⁷V. B. Georgiev, J. Cuenca, F. Gautier, L. Simon, and V. V. Krylov, "Damping of structural vibrations in beams and elliptical plates using the acoustic black hole effect," *J. Sound Vib.* **330**, 11 (2011).
- ³⁸E. Riva, M. I. N. Rosa, and M. Ruzzene, "Edge states and topological pumping in stiffness modulated elastic plates," *Phys. Rev. B* **101**(9), 094307 (2020).
- ³⁹G. Gafforelli, R. Ardito, and A. Corigliano, "Improved one-dimensional model of piezoelectric laminates for energy harvesters including three dimensional effects," *Compos. Struct.* **127**, 369–381 (2015).
- ⁴⁰R. Ardito, A. Corigliano, G. Gafforelli, C. Valzasina, F. Procopio, and R. Zafalon, "Advanced model for fast assessment of piezoelectric micro energy harvesters," *Front. Mater.* **3**, 17 (2016).